THE JOURNAL OF THE ACOUSTICAL SOCIETY OF KOREA Vol.27, No.3E 2008. 9. pp. 104~111

Broadening of Foci in an Ocean Time Reversal Processing and Application to Underwater Acoustic Communicaion

Kee-Cheol Shin*, Jea-Soo Kim**
*Maritime R&D Lab., LIG Nex1 Co., Ltd.
**Department of Ocean Engineering, Korea Maritime University
(Received June 16, 2008; accepted September 16, 2008)

Abstract

Recently, a method for robust time reversal focusing has been introduced to extend the period of stable focusing in time-dependent ocean environments [S. Kim *et al.*, J . Acoust. Soc. Am. 114, 145-157, (2003)]. In this study, concept of focal-size broadening based on waveguide invariant theory in an ocean time reversal acoustics is described. It is achieved by imposing the multiple location constraints. The signal vector used in multiple location constraints are found from the theory on waveguide invariant for frequency band corresponding the extended focal range. The broadening of foci in an ocean waveguide can play an important role in the application of time reversal processing, particularly to the underwater acoustic communication with moving vehicles. The proposed method is demonstrated in the context of the underwater acoustic communication from the transmit/receive array (TRA) to a slowly moving vehicle.

Keywords: *Time reversal processing (TRP), Broadening of foci, Underwater acoustic communication, Multiple location constraints (MLC)*

I. Introduction

It is well known that time reversal processing (TRP) uses the received signal from a probe source to refocus the signal at the probe source location by backpropagating the time-reversed version of the received signal. Since TRP has been implemented in the laboratory [2-3], and in the ocean [4-6], a specific application of TRP to achieve a low-error bit rate in underwater communication has successfully been demonstrated [7]. Further, the concept of adaptive weighting on a transmit/receive array (TRA) before back propagation has been introduced in TRP and referred to as adaptive time reversal processing (ATRP) [8]. Further, multiple focusing using ATRP is applied to the self-equalization process at multiple receiving locations in long-range underwater acoustic communication [9].

The physical principle of the focal size for TRP is the same as that of the matched field processing (MFP) [10]. While a propagation model is used to match the source-generated sound field in MFP, in TRP, the time reversal signal is physically back-propagated to the original source position using a TRA. Hence, the focal size realized by TRP can be considered as the maximum achievable resolution of MFP for given waveguide conditions.

The superior performance of an array in a waveguide over the free-space diffraction limit has already been reported in the context of MFP using Cramer-Rao bounds [10] and in ultrasonic [11] and ocean experiments [4].

The ability to maintain a stable focus is important

Corresponding author: Kee-Cheol Shin (kcshin@lignex1.com)
Maritime R&D Lab., LIG Nex1 Co., Ltd., 102-18, Mabuk-dong, Giheung-gu, Yongin-City, Gyeonggi-do, Korea

in the application of TRP. In underwater acoustic communications, it is desirable to extend the extent and period of reliable communication using a single probe pulse captured for increasing the data rate by increasing the time intervals between the training probe pulses [7]. The analogy between TRP and MFP can provide useful guidance for developing more robust MFP methods [12].

The objective of this study is to develop an efficient method for robust time reversal focusing for broadening the focal size in an ocean waveguide environment. To achieve this, the application of TRP is extended to the broadening of focus in the frequency domain and also determining the time domain solution in an ocean waveguide. The proposed method is demonstrated in the context of underwater acoustic communication from the TRA to an autonomous underwater vehicle (AUV) moving at low speed. The main feature of the proposed method is to increase the immunity to the range mismatch between TRA and a moving source.

In Sec. II, the formulation of TRP is reviewed and the application of TRP is extended to the broadening of foci. Simulation results are presented in Sec. III. The conclusions of the study are presented in Sec. IV.

II. Theory

2.1. Review of time reversal processing

In order to review TRP, we follow the conventions of Ref. [8]. As described in Figure 1, the phase-conjugate field at the field location $\vec{r}$ in the frequency domain is written as

$$P(\vec{r},\omega)=\sum_{n=1}^{N}S^{*}(\omega)g^{*}(\vec{r}_n\,|\,\vec{r}_{ps},\omega)g(\vec{r}\,|\,\vec{r}_n,\omega)$$
$$=S^{*}(\omega)\mathbf{g}^{\dagger}(\mathbf{r}_{array}\,|\,\vec{r}_{ps},\omega)\mathbf{g}(\vec{r}\,|\,\mathbf{r}_{array},\omega) \quad (1)$$

where $S(\omega)$ is the source spectrum and $g(\vec{r}_n\,|\,\vec{r}_{ps})$ is the Green's function at the nth array element location $\vec{r}_n$ propagated from the source position $\vec{r}_{ps}$. Likewise, $g(\vec{r}\,|\,\vec{r}_n)$ is the field propagated from the nth array element location $\vec{r}_n$ to the arbitrary receiver location $\vec{r}$ as shown in Figure 1, where N is the number of array elements and the superscripts $[\,]^{*}$ and $[\,]^{\dagger}$ denote the complex conjugate and Hermitian transpose, respectively. In a vector notation, $\mathbf{g}$ and $\mathbf{r}_{array}$ are $N\times 1$ column vectors. The position vectors are written in italic letters with arrows and the column vectors and matrices are written in boldface letters.

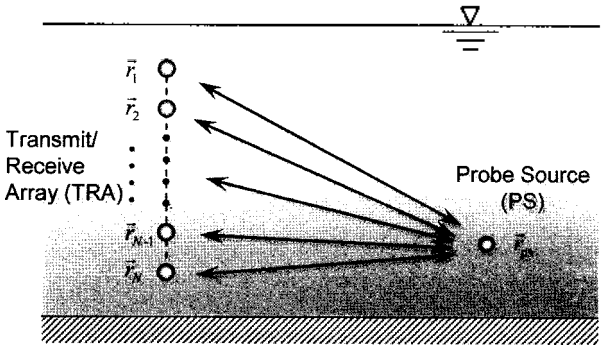

Figure 1. Description of time reversal processing.

2.2. Robust time reversal focusing using multiple location constraints

A simple approach for achieving robust time reversal focusing is to use multiple location constraints (MLC). Ref. [1] provides the theoretical background in detail including MLC and simulations of robust focusing.

The MLC method utilizes multiple neighboring points to construct a backpropagating signal vector from the TRA. In order to apply the MLC method to TRP, we should modify the measured probe signal rather than replica fields since the ocean itself generates the replica fields in TRP. This requires multiple probe signals obtained at different locations, which might not be possible in practice.

The signal vector for MLC is obtained by the waveguide invariant theory, which relates the frequency shift to the focal range shift.

The first step of robust TRP is to construct a probe signal matrix by obtaining multiple probe signal vectors as

$$\mathbf{P}(\omega)=[\mathbf{p}_1,\mathbf{p}_2,\cdots,\mathbf{p}_J] \quad (2)$$

where $\mathbf{P}$ is an $N\times J$ probe signal matrix at frequency ω and each element $\mathbf{P}_j$ is an $N\times 1$ signal vector; N is the number of elements in the TRA and J is the number of probe signal vectors received by the TRA.

In the MLC method, the vectors represent narrow-band signals received from sources in different ranges:

$$\mathbf{p}_j = g(\vec{r}_n \mid \vec{r}_j, \omega) \tag{3}$$

where $g(\vec{r}_n \mid \vec{r}_j, \omega)$ is the Green's function at frequency ω between the TRA at $\vec{r}_n$ and the probe source at $\vec{r}_j$. The known source spectrum $S(\omega)$ is removed from the received signal. The signal vectors should be derived from the ranges of the possible focal shifts near the probe source using the waveguide invariant theory.

The next step is to derive a field vector for back-propagation. The design of an efficient constraint space for the signal vector consists of selecting the minimum number of vectors that can best approximate the phase perturbation space. This dimension reduction can be achieved by the singular value decomposition (SVD) of the signal matrix $\mathbf{P}$ with a rank K approximation:

$$\mathbf{P}(\omega) = \mathbf{U}\Sigma\mathbf{V}^{\dagger} \tag{4}$$

where $\mathbf{U}$ is an $N\times K$ column-orthogonal matrix whose columns are the left singular vectors, Σ is a $K\times K$ diagonal matrix whose elements are the singular values of $\mathbf{P}$, and $\mathbf{V}$ is a $J\times K$ orthogonal matrix whose columns are the right singular vectors. Here, N is the number of receivers in the TRA and J is the number of multiple neighboring points for constructing a backpropagating signal vector from the TRA. The field vector $\mathbf{w}$ for backpropagation can be obtained from a linear combination of the left singular vectors:

$$\mathbf{w}(\omega) = \mathbf{U}(\omega)\mathbf{q} \tag{5}$$

where $\mathbf{q}$ is a $K\times 1$ vector representing the contributions of each singular vector. The singular values tend to decrease rapidly with an increasing number of singular vectors such that the first singular vector corresponding to the largest singular value can be sufficient as a field vector for stable focusing, i.e., $\mathbf{q}=[1,0,\ldots,0]^T$. In other words, the effective rank of $\mathbf{P}$ is equal to one.

The final step is to replace $g(\vec{r}_n \mid \vec{r}_{ps}, \omega)$ in Eq. (1) with $\mathbf{w}(\omega)$ in Eq. (5). Then, the robust time-reversed pressure field becomes

$$\begin{aligned} p(\vec{r},\omega) &= \sum_{n=1}^{N}\left[S^*(\omega)w^*(\vec{r}_n,\omega)\right]g(\vec{r}\mid\vec{r}_n,\omega) \\ &= S^*(\omega)\mathbf{w}^{\dagger}(\omega)\mathbf{g}(\vec{r}\mid\mathbf{r}_{\text{array}},\omega) \end{aligned} \tag{6}$$

This approach should provide an expanded focal structure assuming that the field vector $w^*(\vec{r}_n,\omega)$ is chosen to maintain a high correlation with $g(\vec{r}\mid\vec{r}_n,\omega)$ for expanded ranges of interest.

Finally, the time domain solutions, or the bit sequences to be transmitted from the TRA are found by inverse Fourier transformation. The jth element of the TRA transmits the following time domain solution signal, given by the Fourier synthesis of the bracketed term in Eq. (6).

$$p(t,\vec{r}_j) = \int S^*(\omega)w^*(\vec{r}_j,\omega)e^{-i\omega t}d\omega \tag{7}$$

where $S(\omega)$ is the Fourier transform of the probe source pulse. This expression incorporates all conditions for the broadening of foci at the probe source location.

2.3. Determination of probe signal matrix using waveguide invariant theory

As described earlier, the weight vector usually requires the measurement of the probe signal matrix for the locations near the probe source. The probe signal matrix, however, can be predicted in an acoustic waveguide using the waveguide invariant theory if the broadening is to be carried near the probe source in the range direction.

In a dispersive and multimodal waveguide, the lines of constant sound intensity lead to a constant slope between certain parameters of the waveguide [13-15]. The invariant, denoted by β, characterizes the relation between the range and the frequency as

$$\beta = \frac{R}{\omega}\frac{\delta\omega}{\delta R} \tag{8}$$

where R is the horizontal range and ω is the angular frequency.

For a Pekeris waveguide, the value of β is one; therefore,

$$R' = \frac{\omega'}{\omega}R \tag{9}$$

Eq. (8) states that the acoustic field at (R',ω) approximates the value at (R,ω'). Therefore, the signal vector received at the array can be used to calculate the probe signal matrix near the probe source range at the same depth; therefore, the foci can be broadened without using probe signals.

III. Simulation

In this section, the broadening of focal size is demonstrated in the ocean waveguide. As seen in Figure 2 the vertical TRA consists of 17 elements spanning the 120 m deep water column from 10 to 90 m with 5 m interelement spacing. The probe source is located at 100 m depth and is 3 km away from the TRA. As a propagation model, KRAKEN normal mode program was used throughout the simulation [16].

The transmitted probe pulse has a center frequency f_c=500 Hz and ping duration τ=20 ms which is shown in Figure 3. The sampling frequency is 8192 Hz and the FFT size is 8192; therefore, the time duration is 1.0 s. This time duration is sufficient to prevent aliasing in time due to pulse elongation caused by dispersion.

3.1. Time reversal processing

For the environment described in Figure 2, Figure 4(a) shows the acoustic field in the frequency domain obtained using a probe source at a 100-m depth. The depth-stacked time series received in the TRA are shown in Figure 4(b).

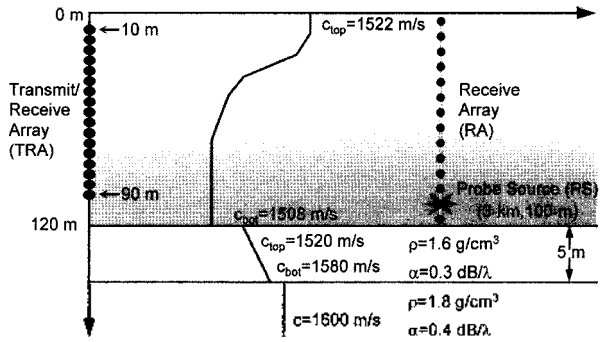

Figure 2. Schematic and parameters of the ocean waveguide used for the simulation.

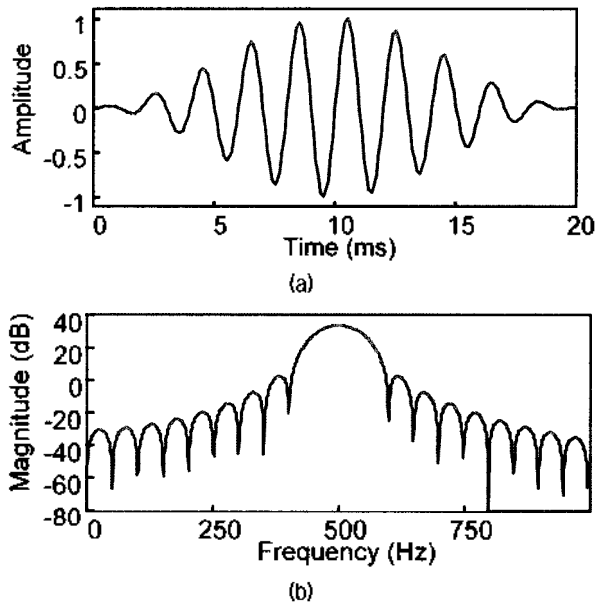

Figure 3. Probe source (a) signal and (b) spectrum.

Figure 4(a) shows the transfer function at a frequency of 500 Hz by considering the ocean as a spatial filter. If the source located at a depth of 100 m transmits a pulse at the carrier frequency of 500 Hz, the time arrival structure at the receivers in the TRA can be evaluated by the Fourier synthesis of frequency solutions over the bandwidth of interest. When the received signal at the TRA is time reversed and back-propagated, the signal focuses back to the probe source location as shown in Figure 4 (c)-(d). Figure 4(c) depicts the propagation from the TRA to the receiver array (RA). In this geometry, the probe source is located at a range of 3 km and depth of 100 m. As expected, the phase conjugation of the 500-Hz frequency component and its consequent propagation through the waveguide produce a spatial focus at the probe

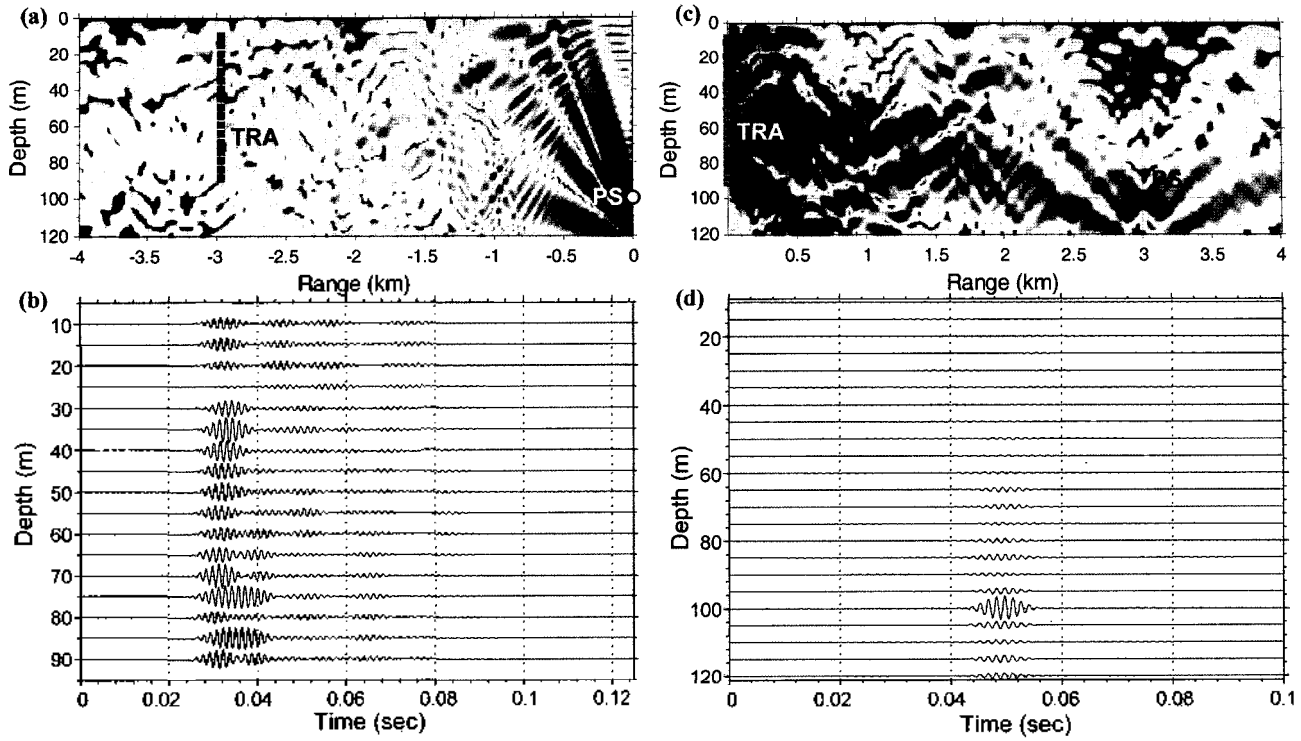

Figure 4. Time reversal simulation. (a) Acoustic field from probe source to TRA, (b) depth-stacked time series received at the TRA using a probe source at 100-m depth, (c) single frequency phase conjugation simulation at 500 Hz: probe source at 100-m depth and 3-km range, (d) depth-stacked time series at 3-km range.

source location. Figure 4(d) shows the time series received at the 3-km range as a function of depth.

3.2. Broadening of focal size

The transfer function at the broadening position is obtained by the waveguide invariant theory, as described in the previous section. Since the broadening is to be carried out in the range between 2.75 and 3.25 km, the frequency of the wave vector to be backpropagated instead of the wave vector with a carrier frequency of 500 Hz can be calculated from Eq. (8) as

$$f' = 500\ \text{Hz} \times \frac{3\ \text{km}}{2.75\ \text{km}} = 545.4545\text{Hz}$$
$$f' = 500\ \text{Hz} \times \frac{3\ \text{km}}{3.25\ \text{km}} = 461.5385\ \text{Hz} \quad (9)$$

Figure 5 shows the broadening of the focal size by robust TRP. 51 signal vectors are calculated using the virtual probe sources evenly distributed in the range between 2.75 and 3.25 km. The focal size is broadened in the range direction by imposing a set of constraints termed the MLC. The signal vectors used in the constraints are determined by the waveguide invariant theory. By this theory, the signal vectors

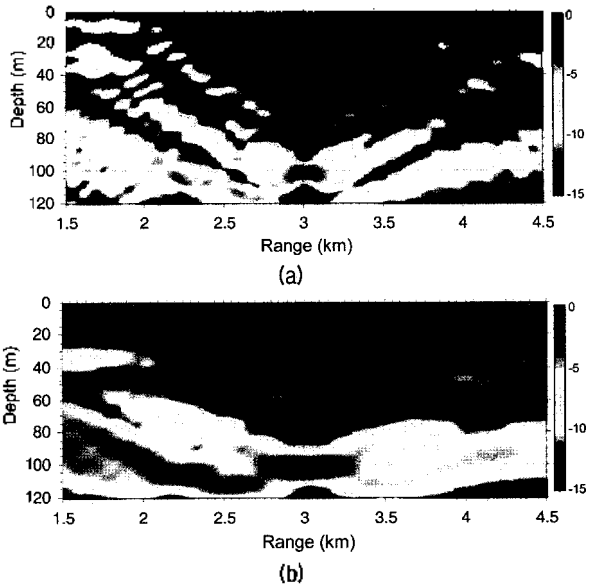

Figure 5. Single frequency phase conjugation simulation at 500 Hz. (a) conventional TRP and (b) robust TRP using MLC, where the additional constraints for broadening of foci are placed in the range between 2.75 and 3.25 km at a depth of 100 m.

near the probe source are considered simply as frequency -shifted signal vectors coming from the source.

IV. Application to Long-Range Underwater Communication

The proposed method can find applications where a robust and broad focal size is desired. In the numerical simulation, the signal transmission of bit sequences for underwater acoustic communication is demonstrated. The nominal signaling rate is 27.2 symbols/sec, and 4 bits of information are encoded in each symbol. The channel used for the numerical simulations is shown in Figure 2.

4.1. Signal scheme

In this signaling scheme, each symbol represents a 4-bit word, which results in a total of 16 different words in the code. Since this communication system is based on noncoherent detection, the value of each bit within a symbol is given by the detection or lack of detection of the corresponding frequency component. There are 15 different symbols in the code having at least one spectral component. The "all-zeros" word corresponds to the case where no carrier frequencies are detected. This signaling scheme corresponds to a four-channel "on-off" keying modulation scheme. In this scheme, four frequency components centered at 300, 400, 500, and 600 Hz are defined. Each one of these frequency components spans 100 Hz in frequency and has a -3 dB bandwidth of 36.6 Hz.

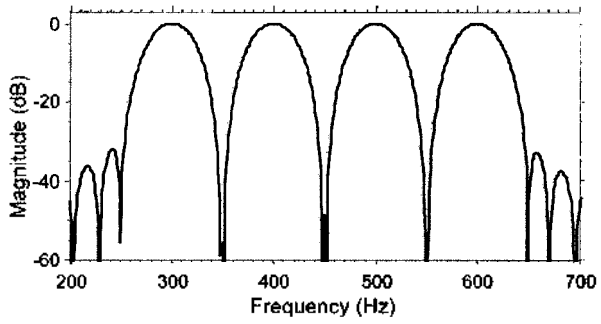

Figure 6. TRA filter bank frequency response.

4.2. Message transmission

This section presents a numerical simulation in which a message is sent from the TRA to the probe source location shown in Figure 2. At each TRA element, the transmitted signal corresponding to a given symbol can be obtained by the time domain superposition of its different frequency components. Similarly, the signal corresponding to a sequence of symbols can be obtained by the superposition of the signals corresponding to different symbols, suitably delayed in the time domain. This time domain delay corresponds to the signaling period and should be greater than the temporal duration of each symbol at the receiver location in order to avoid intersymbol interference. In this case, each single frequency component will have a temporal duration of 36.7 ms, which is chosen as the signaling period.

Figure 7 shows the ideal signal that the TRA intends to focus at the receiver at the probe source location. Figs. 8 and 9 show the message signal spectrograms at various ranges of the signal corresponding to a message composed of a sequence of words from $(0001)_2$ to $(1111)_2$ that is intended to be transmitted from the TRA to the receiver at the probe source location. Here, subscript $(\ )_2$ denotes the base-2 (binary) notation. All the signals are collected at a depth of 100 m. Figs. 8 and 9 show the signal spectrograms obtained at different ranges using conventional TRP and robust TRP, respectively. The displayed data corresponds to the received signals at a depth of 100 m and ranges of 3 km, 2.9 km, and 2.75 km.

When conventional TRP is employed, as shown in Figure 8, one can observe the correct message signal at the probe source location where the multipath structure is greatly suppressed. However, outside the focal region,

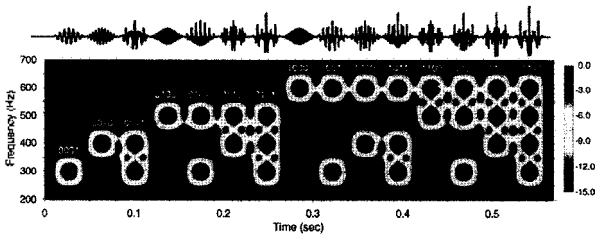

Figure 7. Desired message signal spectrogram if no distortions are present in the channel.

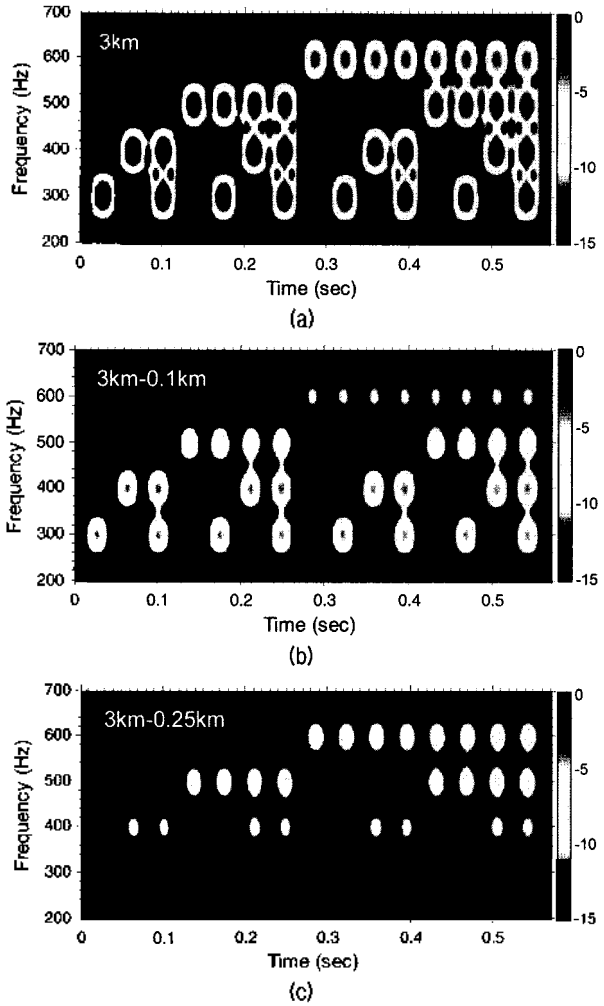

Figure 8. Message signal transmission simulation using conventional TRP.

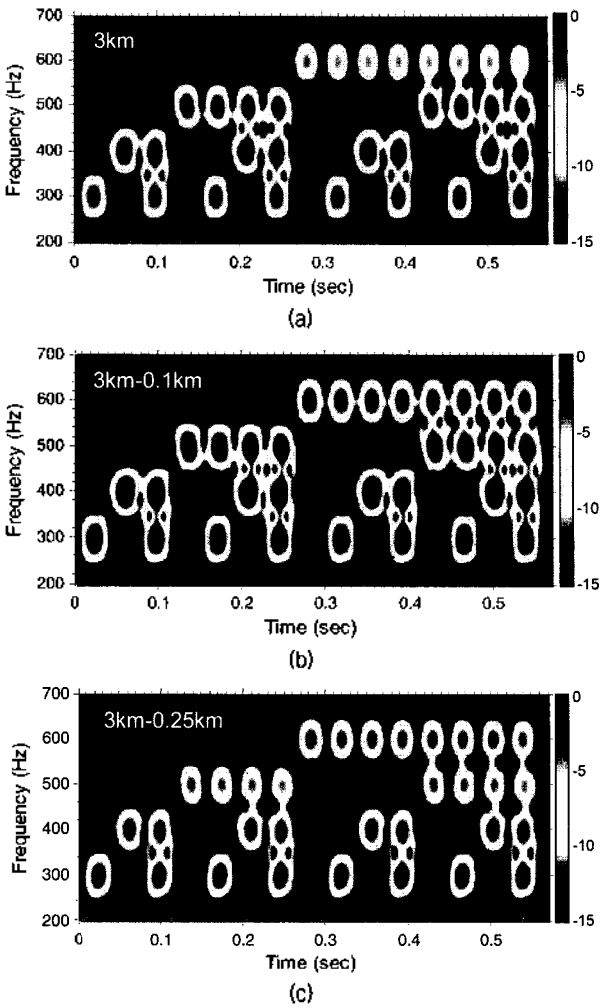

Figure 9. Message signal transmission simulation using robust TRP.

weak message signals are received. Finally, Figure 9 illustrates the broadening of the focal size at various ranges when the MLC method with constraint vectors derived by the waveguide invariant theory is applied to the robust TRP. For the MLC method shown in Figure 9, 51 signal vectors are calculated using the virtual probe sources distributed in the range between 2.75 and 3.25 km. To compare these results with those of the conventional method, the intensity field is normalized. We can observe that highly correlated correct message signals are received in the extended focal region. Therefore, robust TRP with focal size expansion is advantageous for the underwater acoustic communication from the TRA to the vehicle moving at a low speed.

V. Conclusion

This paper describes a way to broaden time reversal focusing in context of ocean acoustics where one source faces a vertical transmit/receive array. The simulation results of underwater communication by QFSK transmission in shallow water are shown. It is shown that the proposed method can find many applications where a robust and broad focal size is desired. The proposed method was applied to a low frequency band with a low data rate in a no noise case simulation scenario. In the future research, we will make the proposed method useful of underwater acoustic communication of practical interest.

Acknowledgments

This work was supported by grant No. R01200 6000113402006 from the Basic Research Program of the Korea Science & Engineering Foundation and Defense Acquisition Program Administration & Agency for Defense Development under the contract UD07 0054AD.

References

1. S. Kim, W. A. Kuperman, W. S. Hodgkiss, H. C. Song, G. F. Edelmann and T. Akal, "Robust time reversal focusing in the ocean," J. Acoust. Soc. Am. **114**, 145–157, 2003.
2. M. Fink, "Time-reversal mirrors," in Acoustical Imaging, B. F. Jones Ed. New York: Plenum, **25**, 1–15, 1995.
3. M. Fink, "Time-reversal acoustics," Phys Today, **50**, 34–40, 1997.
4. W. A. Kuperman, W. S. Hodgkiss, H. C. Song, T. Akal, C. Ferla and D. R. Jackson, "Phase conjugation in the ocean: Experimental demonstration of an acoustic time-reversal mirror," J. Acoust. Soc. Am. 103, 25–40, 1998.
5. H. C. Song, W. A. Kuperman and W. S. Hodgkiss, "A time-reversal mirror with variable range focusing," J. Acoust. Soc. Am. **103**, 3234–3240, 1998.
6. D. R. Jackson and D. R. Dowling, "Phase conjugation in underwater acoustics," J. Acoust. Soc. Am. **89**, 171–181, 1991.
7. G. F. Edelmann, T. Akal, W. S. Hodgkiss, S. Kim, W. A. Kuperman and H. C. Song, "An initial demonstration of underwater acoustic communication using time reversal," IEEE J. Oceanic Eng. **27**, 602–609, 2002.
8. J. S. Kim, H. C. Song and W. A. Kuperman, "Adaptive time-reversal mirror," J. Acoust. Soc. Am. **109**, 1817–1825, 2001.
9. J. S. Kim and K. C. Shin, "Multiple focusing with adaptive time-reversal mirror," J. Acoust. Soc. Am. **115**, 600–606, 2004.
10. A. B. Baggeroer, W. A. Kuperman and H. Schmidt, "Matched field processing: Source localization in correlated noise as an optimum parameter estimation problem," J. Acoust. Soc. Am. **83**, 571–587, 1988.
11. P. Roux and M. Fink, "Time reversal in a waveguide: Study of the temporal and spatial focusing," J. Acoust. Soc. Am. **107**, 2418–2429, 2000.
12. A. B. Baggeroer, W. A. Kuperman and P. N. Mikhalevsky, "An overview of matched field methods in ocean acoustics," IEEE J. Oceanic Eng. **18**, 401–424, 1993.
13. S. D. Chuprov, "Interference structure of a sound field in a layered ocean," Acoustics of the Ocean: Current Status (in Russian), edited by L. M. Brekhovskikh and I. B. Andreevoi, (Nauka, Moscow, 71–91, 1982).
14. G. A. Grachev, "Theory of acoustic field invariants in layered waveguide," Acoust. Phys. **39**, 33–35, 1993.
15. G. L. D'Spain and W. A. Kuperman, "Application of waveguide invariants to analysis of spectrograms from shallow water environments that vary in range and azimuth," J. Acoust. Soc. Am. **106**, 2454–2468, 1999.
16. M. B. Porter, "The KRAKEN Normal Mode Program," SACLANT Undersea Research Center SM-245, La Spezia, Italy, 1991.

[Profile]

• Kee-Cheol Shin

Kee-Cheol Shin received the B.S., M.S. and Ph.D degrees in ocean engineering from the Korea Maritime University, Pusan, Korea, in 1996, 1998 and 2003, respectively. He is currently a Senior Research Engineer at Maritime R&D Lab., LIG Nex1 Company, Youngin, Korea. His current research interests include sonar signal processing, time reversal acoustics, and underwater acoustic communication.

• Jea-Soo Kim

Jea-Soo Kim received B.S. degree from Seoul National University, Seoul, Korea, in 1981, the M.S. degree from University of Florida, Gainsville, in 1984, and the Ph.D. degree from Massachusetts Institute of Technology, Campbridge, in 1989. Since 1991, he was with Korea Maritime University, Pusan, Korea. From 1999 to 2001, he was a Visiting Scholar in MPL/SIO, University of California San Diego.